ANALYTICAL STUDY OF LUNAR LANDING TRAJECTORIES WITH REFERENCE TO THE LUNAR-ORBIT-RENDEZVOUS MODE AND POSSIBLE ABORT SITUATIONS

by James L. Williams and L. Keith Barker

Langley Research Center
Langley Station, Hampton, Va.

NATIONAL AERONAUTICS AND SPACE ADMINISTRATION • WASHINGTON, D. C. • DECEMBER 1963

TECHNICAL NOTE D-2016

ANALYTICAL STUDY OF LUNAR LANDING TRAJECTORIES WITH REFERENCE TO THE LUNAR-ORBIT-RENDEZVOUS MODE AND POSSIBLE ABORT SITUATIONS

By James L. Williams and L. Keith Barker

Langley Research Center
Langley Station, Hampton, Va.

NATIONAL AERONAUTICS AND SPACE ADMINISTRATION

NATIONAL AERONAUTICS AND SPACE ADMINISTRATION

TECHNICAL NOTE D-2016

ANALYTICAL STUDY OF LUNAR LANDING TRAJECTORIES WITH REFERENCE TO THE LUNAR-ORBIT-RENDEZVOUS MODE AND POSSIBLE ABORT SITUATIONS

By James L. Williams and L. Keith Barker

SUMMARY

An analytical investigation has been made of lunar landing trajectories with reference to the lunar-orbit-rendezvous mode and possible abort situations. Landing trajectories from parking orbits at altitudes of 50 international statute miles and 100 international statute miles were computed, and abort capabilities near lander touchdown were studied by consideration of relative angular separation of the orbiter and lander at touchdown. All the landing trajectories utilized two thrusting periods: one to deorbit and another for braking to the lunar surface with zero velocity. Also studied were landing trajectories wherein the lander is placed in a trajectory which has a period equal to that of the parking orbit. In the event of difficulties, such as engine failure, prior to the braking maneuver, the lander would return to the proximity of the orbiter once per orbit for rendezvous or rescue by the orbiting vehicle.

The results of this study show that, in general, long landing ranges and high initial thrust-weight ratios resulted in the lunar excursion vehicle leading the orbiter at touchdown, a condition that appears to be favorable from abort considerations (for direct return to the orbiter). Increasing the parking-orbit altitude from 50 to 100 statute miles provided a greater negative separation angle (lander leading) for a particular landing range and specified initial thrust-weight ratio. High initial thrust-weight ratios resulted in a decrease in characteristic velocity (measure of fuel consumption). The characteristic velocity was slightly higher for landings from a 100-statute-mile-altitude orbit than from a 50-statute-mile-altitude orbit. For a lunar excursion vehicle weighing about 35 percent of the vehicle earth escape weight, the overall mission fuel consumption was insensitive to parking-orbit altitude. The characteristic velocity was somewhat higher for landing from pericynthion of the synchronous orbit than for gravity-turn trajectories having the same initial thrust-weight ratio and landing range; however, synchronous landing trajectories tend to improve the abort capabilities of the lunar excursion vehicle.

INTRODUCTION

Several approaches to performing the manned lunar-landing mission have been under consideration for some time. Of these approaches the lunar-orbit-rendezvous mode has been selected by this nation as the primary method of accomplishing the lunar exploration mission. In this mode the space vehicle that departs from earth establishes a close orbit around the moon. This vehicle consists of three major components: a service module (SM), a control module (CM), and a lunar excursion module (LEM). After the lunar parking orbit is established, the LEM separates from the other modules and performs the actual landing. When the landing and exploration are complete, the LEM will rendezvous with the CM and SM. The LEM crew and possibly certain scientific equipment are then transferred to the CM; the LEM is then jettisoned, and the crew returns toward earth in the control and service modules. The phases described above are shown schematically in figure 1.

The lunar-orbit-rendezvous mode, as the name implies, involves a rendezvous in lunar orbit. There have been a number of studies to determine the implications of the required rendezvous on various phases of the lunar mission. A summary of some of these studies is given in reference 1. One phase of the mission which has not received sufficient attention is that of selection of parking-orbit altitude and subsequent landing trajectories from the viewpoint of possible abort situations. The purpose of this paper, therefore, is to examine this phase in some detail.

SYMBOLS

Where distances are expressed in miles, the statute mile is intended. The following factors are included for use in converting English units:

1 international statute mile = 0.8689762 international nautical mile

1 international foot = 0.3048 meter (exact)

F	thrust, lb
g_e	gravitational acceleration at surface of earth, 32.2 ft/sec^2
g_m	gravitational acceleration at surface of moon, 5.32 ft/sec^2
h	altitude, ft or statute miles
I_{sp}	specific impulse, 420 sec
i	mission phase (may be any of 1 to 6)
M_H	mass on approach hyperbolic trajectory
M'	mass of command and service modules in circular parking orbit, slugs

M_6' mass injected into earth return, slugs

m mass of lander at any point in landing trajectory, slugs

m_f mass of fuel used, slugs

$$m_{f,total} = \sum_{i=1}^{6} m_{f,i}$$

m_o initial mass of lander in parking orbit or at lunar surface, slugs

Q,K intersection points of synchronous transfer orbit and parking orbit, respectively

P semilatus rectum, ft

r radial distance from center of moon, ft

$\dot{r}$ radial velocity component, ft/sec

$\ddot{r}$ radial acceleration, ft/sec^2

r_m radius of moon, 5,702,000 ft

t time, sec or min

t_f time during which rocket is firing, sec

V total velocity, ft/sec

V_e effective exhaust velocity, 13,524 ft/sec

ΔV characteristic velocity, $I_{sp}g_e \log_e \frac{m_o}{m_o - m_f}$, ft/sec

W_o initial weight of lander in lunar parking orbit or at lunar surface, $m_o g_e$, lb

β thrust vector angle (measured from local horizontal), deg or radians

γ vehicle flight-path angle, deg

ϵ orbital eccentricity

θ angular travel over lunar surface, deg or radians

$\dot{\theta}$ angular rate, radians/sec

$\ddot{\theta}$ angular acceleration, $radians/sec^2$

$\Delta\theta$ separation angle between the orbiter (control module and service module) and lander (lunar excursion module) at touchdown, deg

Subscripts:

c circular

H hyperbolic approach

L landing module

p pericynthion

T synchronous transfer orbit

1 braking from hyperbolic approach into circular parking orbit

2 deorbit

3 touchdown

4 lift-off

5 rendezvous

6 inject into earth return

ANALYSIS

An examination is made of the parking-orbit altitude and subsequent landing trajectories from the viewpoint of suitability for possible abort situations. All computations of this investigation were made for a point mass moving in a plane. It was assumed that all maneuvers were made close to the moon so that it was necessary to include only the lunar gravity and vehicle thrust forces in the equations of motion. It was further assumed that the moon was a homogeneous sphere having a radius of 5,702,000 feet and a surface gravity of 5.32 feet per second per second.

The following equations of motion were used:

$$\ddot{r} - r\dot{\theta}^2 = \frac{F}{m} \sin \beta - g_m\left(\frac{r_m}{r}\right)^2 \tag{1}$$

$$r\ddot{\theta} + 2\dot{r}\dot{\theta} = -\frac{F}{m} \cos \beta \tag{2}$$

where

$$m = m_o + \int \dot{m}\, dt_f \tag{3}$$

and

$$\dot{m} = - \frac{F}{g_e I_{sp}} \tag{4}$$

These equations were solved on an electronic digital computer. An iteration process was used to obtain the desired end conditions of zero velocity at touchdown. In the coast phases (no thrust applied) the standard orbit equations were used to determine orbit characteristics at various altitudes. The directions of the angles and vectors are shown in figure 2.

Abort situations are considered in terms of angular separation of the lunar excursion module at touchdown and the orbiting vehicle since this angle is a primary factor in determining the ease with which the lander can return to the orbiter.

The angular separation of the landing module and the orbiting vehicle depends on a number of factors including parking-orbit altitude, type of landing maneuver used, and the acceleration levels used in landing. The computations of this study were based on either a 50-international-statute-mile- or a 100-international-statute-mile-altitude circular parking orbit. Two basically different types of landing maneuvers were used. In one type, the maneuver is initiated by applying a small amount of retrothrust in orbit. The vehicle then coasts to a lower altitude where braking thrust is applied and maintained at a constant level to perform a soft landing. Both the deorbit and braking phases are accomplished with the same constant thrust level, and the thrust is applied against the velocity vector. Some of the computed trajectories are such that lunar impact will occur if the thrust engine fails to restart for the braking maneuver. Such trajectories may not be of interest in actual missions but are included herein for completeness in range of variables studied. The lunar surface range traversed in this landing maneuver is primarily a function of the thrust level used and the length of the deorbit thrust period. This type of landing maneuver was examined in reference 2 for trajectories starting from a 50-mile-altitude parking orbit. In the present study landing trajectories were obtained for initial thrust-weight ratios of 0.28, 0.43, 0.64, 1.00, and 2.00. From these trajectories the angular difference between the orbiting vehicle and the lander at touchdown was obtained along with fuel consumption and other pertinent information. A constant-thrust restartable engine with a specific impulse of 420 seconds was assumed for all computations; however, for purposes of comparison a few results are presented for a specific impulse of 310 seconds.

In the second type of landing trajectory examined, the landing vehicle first establishes an elliptic orbit having the same period as the parking orbit by thrusting in a direction almost along the radius vector ($\beta = -88^\circ$). This equiperiod or synchronous orbit has about a 60,000-foot pericynthion altitude (fig. 3.)

Equations relating the various parameters involved in establishing synchronous orbits are given in appendix A. The braking for the landing maneuver (gravity turn) is initiated from the 60,000-foot pericynthion altitude. One attractive feature of the synchronous orbit is that, if the landing engine fails to start, the lander automatically returns to the proximity of the orbiter once per orbit and is in position for rendezvous with or rescue by the orbiting vehicle.

In this study it was assumed that the earth-moon trajectories from which the lunar orbits were established were 60-hour hyperbolic trajectories. The values of the velocity and altitude at pericynthion for the approach hyperbolic trajectories are shown in figure 4. Also shown in this figure is the circular-orbit velocity associated with each altitude.

RESULTS AND DISCUSSION

There are a number of landing trajectory characteristics which are of interest in considering the requirements for rendezvous and possible abort situations. These characteristics are discussed in this section.

Landing Trajectories

Selected landing trajectories are presented in figure 5 in the form of altitude plotted against angular range for values of F/W_o of 0.28 and 2.00. Results are given for landings from a 50-mile-altitude parking orbit in figure 5(a) and from a 100-mile-altitude parking orbit in figure 5(b). Two trajectories are presented for each value of F/W_o. Associated with each trajectory is a particular value of deorbiting thrusting period $t_{f,2}$. The curves indicate that for a given thrust level the landing range is a function of the deorbiting thrusting period. This effect is shown clearly in figure 6 in which the deorbiting thrusting period is plotted against angular travel over the lunar surface for all values of F/W_o used in this investigation. It can be seen from this figure that for a given value of F/W_o prolonging the deorbiting thrusting period $t_{f,2}$ decreases the angular range.

Separation Angle Between Lander and Orbiter

Probably the most critical time to abort during the landing maneuver occurs when the lander nears the lunar surface with zero velocity. At this time the angular separation of the lander and the orbiter gives a crude indication of the abort situation. It appears desirable that the angular separation be relatively small or that the lander actually lead the orbiting vehicle. (See ref. 3.)

The effect of F/W_o on the separation angle at lander touchdown can be seen in figure 7. This figure presents the separation angle plotted against landing range for values of F/W_o and for landings initiated from 50- and 100-mile-altitude parking orbits. Of particular interest from abort considerations are the

values of separation angle equal to or less than zero (negative $\Delta\theta$) since a negative value of $\Delta\theta$ indicates that the lander leads the orbiter at touchdown. The curves show that long landing range and high F/W_o tend to place the lander ahead of the orbiter at lander touchdown.

The curves of $\Delta\theta$ vary almost linearly with landing range for a given thrust-weight ratio. The slopes of the $\Delta\theta$ curves are somewhat greater for landings from a 100-mile-altitude orbit than those for landings from a 50-mile-altitude orbit. Landings from a 100-mile-altitude orbit appear to be more favorable for abort situations than do the landings from a 50-mile-altitude orbit since they provide a greater negative separation angle (lander leading) for a particular landing range and specified F/W_o.

Some preliminary calculations of ascent trajectories for 50- and 100-mile-altitude orbits have shown that for $F/W_o \geq 1.00$ the ascent trajectories are nearly duplicates of the landing trajectories. Therefore, the curves of figure 7 can be used to determine available landing ranges which permit direct return to the orbiter for given combinations of F/W_o for landing and for ascent. As an example, assume a landing F/W_o of about 0.43, an ascent F/W_o of 2.0, and a 100-mile-altitude parking orbit. In this example the lander could have an angular travel of 63° and use about 180° to return to the orbiter. The lander could also have a value of θ_L of 180° and use only 69° to return to the orbiter. Thus, the available landing range is from $\theta_L = 63^\circ$ to $\theta_L = 180^\circ$ (this assumes no hovering). Note that for the same initial thrust-weight ratios for landing and ascent ($F/W_o = 0.43$ and 2.0) from a 50-mile-altitude orbit the landing range is closely restricted to $\theta_L = 180^\circ$.

The curves of figure 7 can also be used to determine the hovering time permissible if direct ascent to rendezvous is to be accomplished and if the landing and ascent values of F/W_o are specified. For this condition it is necessary to remember that the orbiting vehicle is moving at about 3° angular travel per minute for a 100-mile-altitude orbit and slightly more for a 50-mile-altitude orbit. For example, if a 100-mile-altitude parking orbit is assumed, a landing F/W_o of 0.43, an ascent F/W_o of 2.00, and a landing range θ_L of 180° would mean a lead separation angle of 1.8° near touchdown. If a 180° ascent trajectory is to be used, the lander can gain about 9° on the orbiter. The permissible hovering or stay time for direct ascent therefore is $\frac{9 + 1.8}{3} = 3.6$ minutes. Alternately, if the hovering time is specified, then the range of the ascent maneuver can be determined.

The separation angles for landings using a synchronous transfer orbit are also shown in figure 7 ($F/W_o = 0.43$). Generally, for both the 50- and 100-mile-altitude parking orbits the synchronous landing trajectories tend to improve the abort capabilities of the lunar excursion vehicle in that a negative separation angle was obtained for 100-mile-altitude results (fig. 7) and a large reduction in orbiter lead angle was obtained for the 50-mile altitude (compared with gravity turns for the same F/W_o and landing range). In addition, it is of interest to

point out that the synchronous orbit results for the 50-mile orbit are similar to a value of F/W_o of 0.64 and for the 100-mile orbit to a value of F/W_o of 2.0. A few results are also presented in figure 7 for a specific impulse of 310 seconds. For those values of F/W_o considered, the effect of specific impulse on the angular separation of lander and orbiter was not appreciable.

Characteristic Velocity

The selection of a landing trajectory will be influenced not only by abort considerations but also by the characteristic velocity (a measure of the fuel requirements) for a particular trajectory. The characteristic velocity ΔV for landings initiated from 50- and 100-mile parking orbits can be seen in figure 8 as a function of F/W_o and angular landing range. The following results can be noted from a study of this figure. First, for landings at a constant value of θ_L the characteristic velocity decreases as F/W_o increases. Second, for a given value of F/W_o, the characteristic velocity is slightly higher for landings from a 100-mile-altitude orbit than for landings from a 50-mile-altitude orbit. Third, the characteristic velocities associated with landings from the pericynthion of the synchronous orbits are somewhat higher than those for the gravity-turn trajectories having the same F/W_o (0.43) and range. This is due primarily to the impulse required to establish the synchronous orbit.

Also shown in figure 8 are the results obtained from impulsive ($F/W_o = \infty$) considerations. A landing range of 180° on the impulsive curve corresponds to the familiar Hohmann transfer (minimum fuel consumption). It is of interest to note that the fuel consumption for a given F/W_o does not vary appreciably for landing ranges greater than about 40° and for the higher F/W_o values does not differ appreciably from Hohmann transfer value.

The computations of this paper were made for a specific impulse of 420 seconds. However, results of a few computations made for a specific impulse of 310 seconds indicate that the effect of specific impulse on the characteristic velocity for the landing maneuver is small for F/W_o of 0.43 and above (fig. 8).

As mentioned previously, the landing maneuver from either a 50- or a 100-mile-altitude orbit shows little difference in characteristic velocity (or fuel consumption). It is of interest however to examine the effect of parking-orbit altitude on the overall lunar-mission fuel requirements. A brief study, assuming impulsive thrust, is included in appendix B to examine this area. The more pertinent results are shown in figure 9 which gives the total fuel required for the lunar mission as a function of the lander weight relative to the vehicle earth escape weight at several lunar-orbit altitudes. The figure shows that for relatively light landers a high parking orbit is more economical; whereas, if the lander weight is a large percent of the vehicle earth escape weight, a low orbit is more economical. If the lander weight is about 35 percent of the earth escape weight, the fuel consumption is insensitive to orbit altitude.

Time Required for Landing

The total time required for the landing maneuver from a 50- and from a 100-statute-mile-altitude orbit is shown in figure 10 as a function of landing range for various values of F/W_o. The curves of landing time vary almost linearly with angular range; this linear variation indicates that the average velocity is about the same for all trajectories generated for a given thrust level. This is true for the values of θ_L shown in figure 10 because coasting makes up a large part of the trajectory. The curves also show that the time required for the landing maneuver which covers a given range decreases as F/W_o increases. In addition, the decrease in time is essentially independent of total range.

Thrusting Time Requirements

In general, the trajectories of this study involve two thrusting periods: one to deorbit and the other (a substantially longer thrusting period) to perform braking at landing. The final thrusting time required of the engine for each landing is of interest since certain types of engines have thrusting time restrictions because of cooling problems. In figure 11 is presented the final thrusting period $t_{f,3}$ as a function of landing range θ_L for various thrust-weight ratios. As expected, these results show that the final thrusting period increases as F/W_o decreases. In addition, little dependence of thrusting time on range was apparent above 80^o of angular travel in landing.

CONCLUSIONS

An analytical investigation has been made of lunar landing trajectories with reference to the lunar-orbit-rendezvous mode and possible abort situations. Landing trajectories from 50-statute-mile- and 100-statute-mile-altitude parking orbits were computed, and abort capabilities near lander touchdown were studied by consideration of relative angular separation of the orbiter and lander at touchdown. All the landing trajectories utilized two thrusting periods: one to deorbit and another for braking to the lunar surface with zero velocity. Also studied were landing trajectories wherein the lander is placed in a trajectory which has a period equal to that of the parking orbit. In the event of difficulties, such as engine failure, prior to the braking maneuver, the lander would return to the proximity of the orbiter once per orbit for rendezvous or rescue by the orbiting vehicle.

The following conclusions were indicated by this investigation:

1. In general, long landing ranges and high initial thrust-weight ratios result in the lunar excursion vehicle leading the orbiter at touchdown, a condition that appears to be favorable from abort considerations (for direct return to orbiter).

2. Increasing the parking-orbit altitude from 50 to 100 statute miles provides a greater negative separation angle (lander leading orbiter at touchdown) for a particular landing range and specified initial thrust-weight ratio.

3. High initial thrust-weight ratios result in a decrease in characteristic velocity (fuel consumption). The characteristic velocity is slightly higher for landings from 100-statute-mile-altitude orbits than from 50-statute-mile-altitude orbits.

4. For a lunar excursion vehicle weighing about 35 percent of the vehicle earth escape weight, the overall mission fuel consumption is insensitive to parking-orbit altitude.

5. The characteristic velocity is somewhat higher for landing from pericynthion of the synchronous orbit than that for gravity-turn trajectories having the same initial values of thrust weight ratio and range; however, synchronous landing trajectories tend to improve the abort capabilities of the lunar excursion vehicle.

Langley Research Center,
National Aeronautics and Space Administration,
Langley Station, Hampton, Va., July 26, 1963.

APPENDIX A

DERIVATION OF SYNCHRONOUS ORBIT EXPRESSIONS

The magnitude and direction of the instantaneous velocity increment required to transfer a lunar space vehicle from an initial circular orbit of radius r_c to a synchronous coplanar orbit having a specified pericynthion radius r_p, where r_p is less than r_c, may be expressed as functions of r_p and r_c.

Assume that the problem is defined by the Keplerian two-body equations and that the direction of flight is the same in both orbits (counterclockwise). The magnitude of the impulsive velocity associated with orbit transfer initiated at the arbitrary intersection point Q (see fig. 3) is given by the law of cosines as

$$\Delta V^2 = V_{T,Q}{}^2 + V_c{}^2 - 2V_{T,Q}V_c \cos \gamma_{T,Q} \tag{A1}$$

where the subscripts T, c, and Q refer to the transfer orbit, circular orbit, and point Q, respectively. Equiperiod orbits must have equal energy levels and therefore have equal major axes. The total velocity at any point in an orbit is given by

$$V^2 = g_m r_m{}^2 \left(\frac{2}{r} - \frac{1}{a}\right)$$

where a is the semimajor axis of the orbit. Therefore, at point Q the velocities $V_{T,Q}$ and V_c are equal. Consequently, equation (A1) reduces to

$$\Delta V = \left[2V_c{}^2\left(1 - \cos \gamma_{T,Q}\right)\right]^{1/2} \tag{A2}$$

The corresponding direction angle β (see fig. 3) of the impulsive velocity is expressible as a function of the flight-path angle $\gamma_{T,Q}$ from geometric considerations as

$$\left|2\beta\right| = 180 - \left|\gamma_{T,Q}\right| \tag{A3}$$

Taking the cosine of both sides of equation (A3) and simplifying gives

$$\left|\beta\right| = \cos^{-1}\left[\frac{1}{2}\left(1 - \cos \gamma_{T,Q}\right)\right]^{1/2} \tag{A4}$$

The restriction on the flight directions in the orbits limits the angle β as follows:

$$-\frac{\pi}{4} > \beta > -\frac{\pi}{2} \tag{A5}$$

Using the equality of the semimajor axes of the transfer orbit to the initial circular radius, that is, $a = r_c$, the semilatus rectum and the eccentricity of the transfer orbit may be expressed as

$$P_T = r_c\left(1 - \epsilon_T^2\right) \tag{A6}$$

and

$$\epsilon_T = \frac{r_c - r_p}{r_c} \tag{A7}$$

Substitution of equation (A7) into equation (A6) gives

$$P_T = r_p\left(2 - \frac{r_p}{r_c}\right) \tag{A8}$$

The semilatus rectum may also be represented by

$$P_T = a \cos^2\gamma_{T,Q} \tag{A9}$$

Replacing a by r_c in equation (A9) and equating equations (A9) and (A8) gives upon solving for $\cos \gamma_{T,Q}$

$$\cos \gamma_{T,Q} = \left[\frac{r_p}{r_c}\left(2 - \frac{r_p}{r_c}\right)\right]^{1/2} \tag{A10}$$

Now, substitution of equation (A10) into equations (A2) and (A4), respectively, results in the following expressions:

$$\Delta V = \sqrt{2V_c^2\left\{1 - \left[\frac{r_p}{r_c}\left(2 - \frac{r_p}{r_c}\right)\right]^{1/2}\right\}} \tag{A11}$$

where $V_c^2 = g_m \frac{r_m^2}{r_c}$ and

$$\left|\beta\right| = \cos^{-1}\left\{\frac{1}{2} - \frac{1}{2}\left[\frac{r_p}{r_c}\left(2 - \frac{r_p}{r_c}\right)\right]^{1/2}\right\}^{1/2} \tag{A12}$$

For a specified pericynthion r_p of the synchronous transfer orbit, equations (A11) and (A12) (with appropriate restrictions on β) readily give the corresponding values of ΔV and β required to effect the transfer from a given circular orbit of radius $r_c > r_p$, with the restriction that motion in both orbits is in the same direction.

Although the expressions (A11) and (A12) were derived for the intersection point Q, it is understood that identical expressions can be derived for point K. However, if injection occurs at point K, the angle β is limited between $\pi/2$

and $\pi/4$. It should be pointed out that an exact lower limit of β from a practical viewpoint can be obtained by replacing r_p by r_m in equation (A12) for a given circular orbit. All values of β less than this value result in a synchronous orbit which intercepts the lunar surface.

A useful connection formula between ΔV and β can be obtained by combining equations (A2) and (A4) as

$$\Delta V = 2V_c \cos \beta \tag{A13}$$

where β is restricted by flight direction and r_m. Thus, any combination of equations (A11), (A12), and (A13) can be used to determine the magnitude and direction of the instantaneous velocity increment required to transfer from an initial circular orbit to a synchronous orbit having a specified pericynthion r_p $(r_p < r_c)$.

It is of interest to determine the intersection angles θ_K and θ_Q which are measured counterclockwise from the pericynthion r_p of the synchronous orbit to the intersection points K and Q. Since the radius vectors of the two orbits are equal at the intersection points and $a = r_c$, the intersection angles θ_K and θ_Q may be expressed as

$$\cos \theta_Q = \cos \theta_K = \left(\frac{P_T}{r_c} - 1\right)\frac{1}{\epsilon_T} \tag{A14}$$

Substituting equation (A6) into equation (A14) reduces the expression to

$$\cos \theta_Q = \cos \theta_K = -\epsilon_T \tag{A15}$$

From consideration of equation (A6)

$$\frac{\pi}{2} < \theta_K < \pi \tag{A16}$$

Also,

$$\theta_Q = 360 - \theta_K \tag{A17}$$

and

$$\epsilon_T = 1 - \frac{r_p}{r_c} \tag{A18}$$

Therefore, the intersection angles have been clearly defined. The intersection angles being defined permit the location of the pericynthion r_p above any specified position on the lunar surface by varying the point of application of ΔV along the circumference of the circular orbit.

APPENDIX B

DERIVATION OF EXPRESSIONS FOR THE LUNAR-MISSION FUEL CONSUMPTION

It is desired to derive the expression for the total fuel consumption required to perform the lunar mission depicted in figure 1 as a function of impulsive velocity increment and initial lander mass. The impulsive velocity increment required to establish a circular orbit at pericynthion position is

$$\Delta V_1 = V_{H,p} - V_c$$

where $V_{H,p}$ is the hyperbolic velocity at pericynthion and V_c is the circular velocity of an orbit. Let the mass on the approach hyperbolic trajectory be defined by M_H; then, the final mass after establishing circular orbit can be expressed as

$$M_1 = M_H e^{-\Delta V_1/V_e} \tag{B1}$$

where V_e is a constant. The fuel used in performing the circularizing maneuver impulsively (phase 1) is

$$m_{f,1} = M_H - M_1 \tag{B2}$$

At some position in the circular orbit the lander performs a deorbiting maneuver. Let the velocity decrease during deorbiting be equal to ΔV_2 and the initial mass of the lander in the parking orbit be defined by m_o. Then the mass of the lander after deorbiting is

$$m_2 = m_o e^{-\Delta V_2/V_e} \tag{B3}$$

and the corresponding fuel consumption is

$$m_{f,2} = m_o - m_2 \tag{B4}$$

The impulsive velocity increment required for zero velocity at the lunar surface is equal to ΔV_3. The lander mass after touchdown is

$$m_3 = m_2 e^{-\Delta V_3/V_e} \tag{B5}$$

and the fuel consumed can be written as

$$m_{f,3} = m_2 - m_3 \tag{B6}$$

For lander take-off from the lunar surface an impulsive velocity increment ΔV_4 is defined. The final lander mass after take-off is

$$m_4 = m_3 e^{-\Delta V_4/V_e} \tag{B7}$$

and the corresponding fuel consumption can be expressed as

$$m_{f,4} = m_3 - m_4 \tag{B8}$$

At orbital altitude intercept let the impulse velocity increment required to place the lander in orbit with the appropriate velocity be ΔV_5; then, the mass of the lander is

$$m_5 = m_4 e^{-\Delta V_5/V_e} \tag{B9}$$

and the fuel consumed is

$$m_{f,5} = m_4 - m_5 \tag{B10}$$

If the mass of the space vehicle in the circular parking orbit is defined as

$$M' = M_H - m_{f,1} - m_o \tag{B11}$$

and the velocity required for injection in an earth return trajectory is denoted by ΔV_6, then the vehicle mass on the return trajectory is

$$M_6' = M' e^{-\Delta V_6/V_e} \tag{B12}$$

and the fuel consumed is

$$m_{f,6} = M' - M_6' \tag{B13}$$

The total fuel consumed for the entire lunar mission can be written as

$$m_{f,\text{total}} = \sum_{i=1}^{6} m_{f,1} \tag{B14}$$

Substituting in equation (B14) for the individual fuel consumption gives the following equation for total fuel as a function of initial weight on the hyperbolic orbit, initial lander weight, and the impulsive velocity increments:

$$m_{f,\text{total}} = M_H - M_H e^{\frac{-(\Delta V_1+\Delta V_6)}{V_e}} + m_o e^{-\Delta V_6/V_e} - m_o e^{\frac{-(\Delta V_2+\Delta V_3+\Delta V_4+\Delta V_5)}{V_e}} \tag{B15}$$

Consideration of the symmetric aspects of the impulsive landing trajectory and the impulsive rendezvous trajectory leads to the following definitions:

$$\left.\begin{aligned} \Delta V_1 &= \Delta V_6 \\ \Delta V_3 &= \Delta V_4 \\ \Delta V_2 &= \Delta V_5 \end{aligned}\right\} \tag{B16}$$

Substituting expressions (B16) into equation (B15) and dividing by M_H gives

$$\frac{m_{f,total}}{M_H} = 1 - e^{-2\Delta V_1/V_e} + \frac{m_o}{M_H}\left[e^{-\Delta V_1/V_e} - e^{-2(\Delta V_2+\Delta V_3)/V_e}\right] \tag{B17}$$

REFERENCES

1. Houbolt, John C., Bird, John D., and Queijo, Manuel J.: Guidance and Navigation Aspects of Space Rendezvous. Proceedings of the NASA-University Conference on the Science and Technology of Space Exploration, Vol. 1, NASA SP-11, 1962, pp. 353-366. (Also available as NASA SP-17.)

2. Queijo, M. J., and Miller, G. Kimball, Jr.: Analysis of Two Thrusting Techniques for Soft Lunar Landings Starting From a 50-Mile Altitude Circular Orbit. NASA TN D-1230, 1962.

3. White, Jack A.: A Study of Abort From a Manned Lunar Landing and Return to Rendezvous in a 50-Mile Orbit. NASA TN D-1514, 1962.

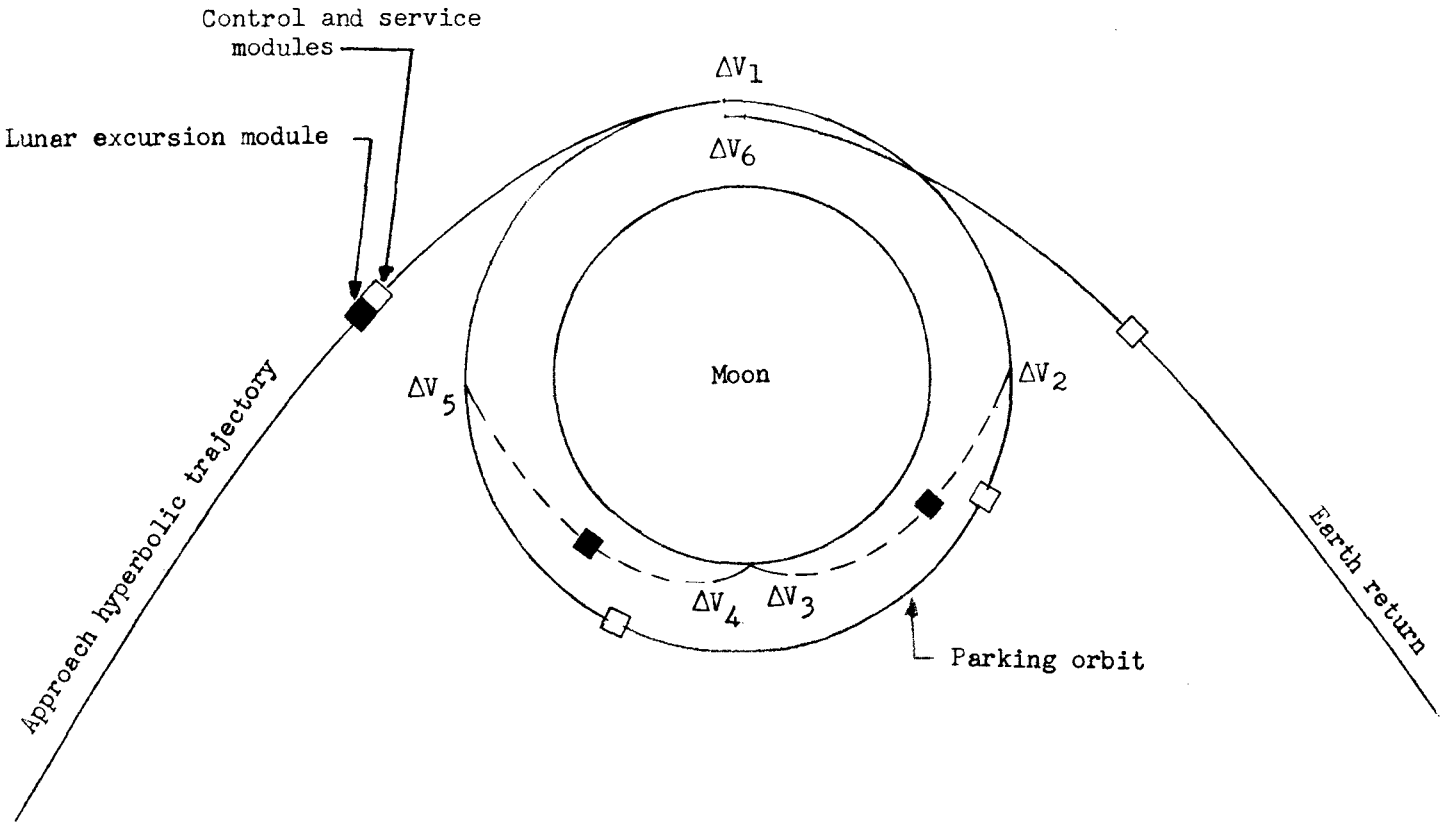

IMPULSIVE VELOCITY	FUNCTION
$\Delta V_1 = \Delta V_6$	Establish parking orbit and inject control module into earth return
$\Delta V_2 = \Delta V_5$	Deorbit excursion module and reestablish parking orbit (rendezvous)
$\Delta V_3 = \Delta V_4$	Lunar touchdown and lift-off of excursion module

Figure 1.- Lunar-mission scheme used to study fuel consumption as a function of the weight of the excursion module and parking-orbit altitude.

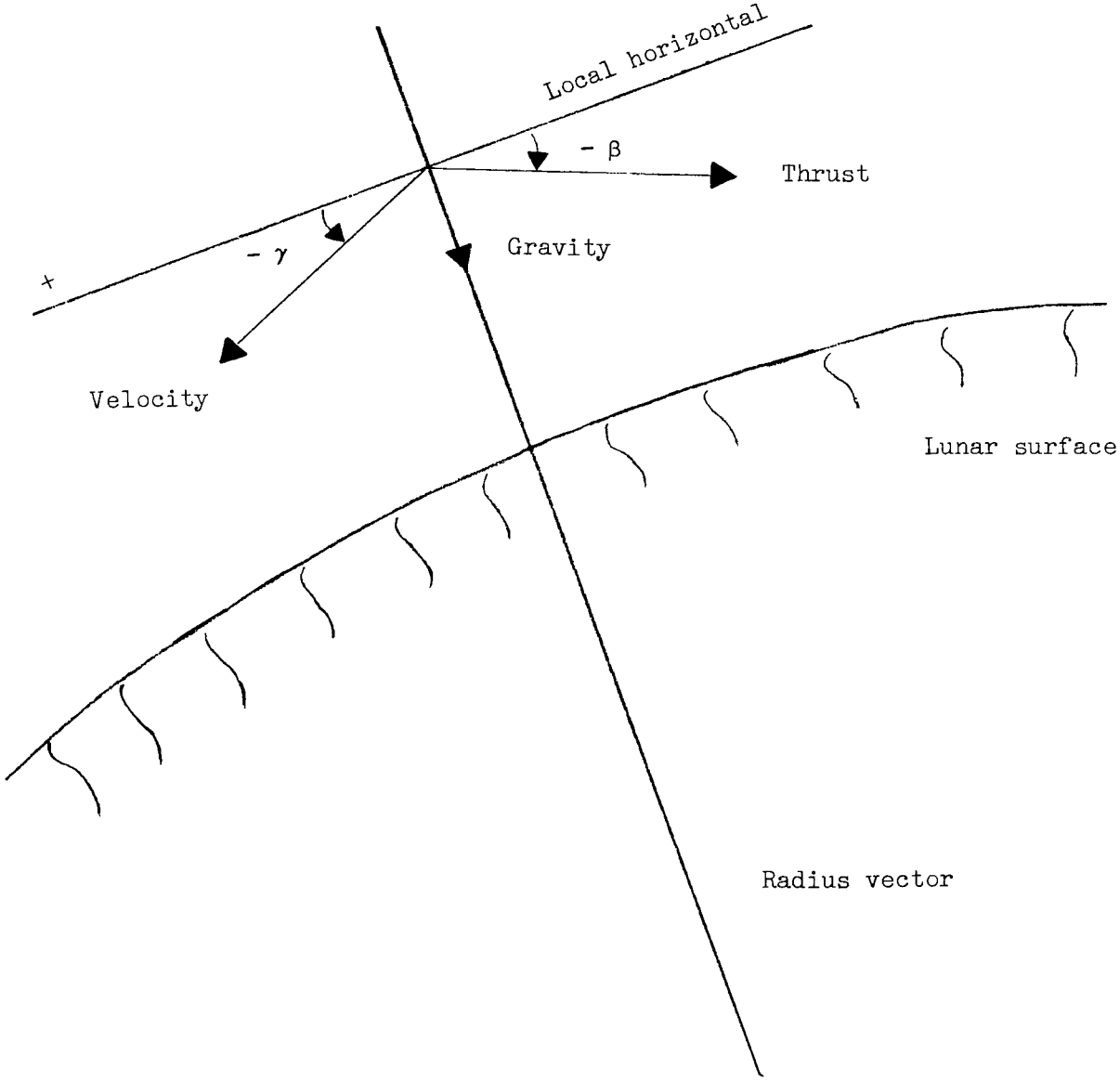

Figure 2.- Illustration of angles and vectors.

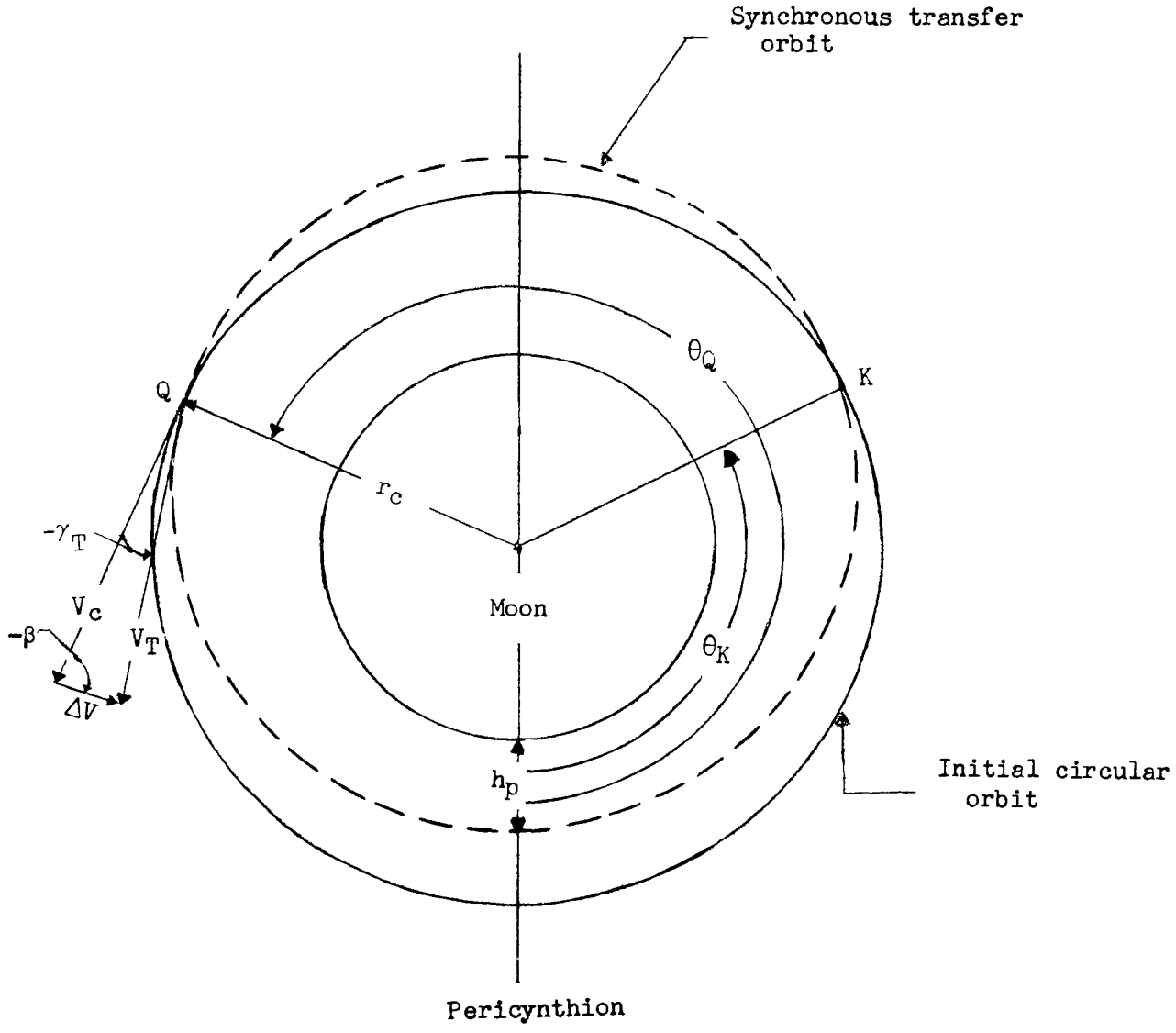

Figure 3.- Establishment of a synchronous transfer orbit from an initial circular orbit.

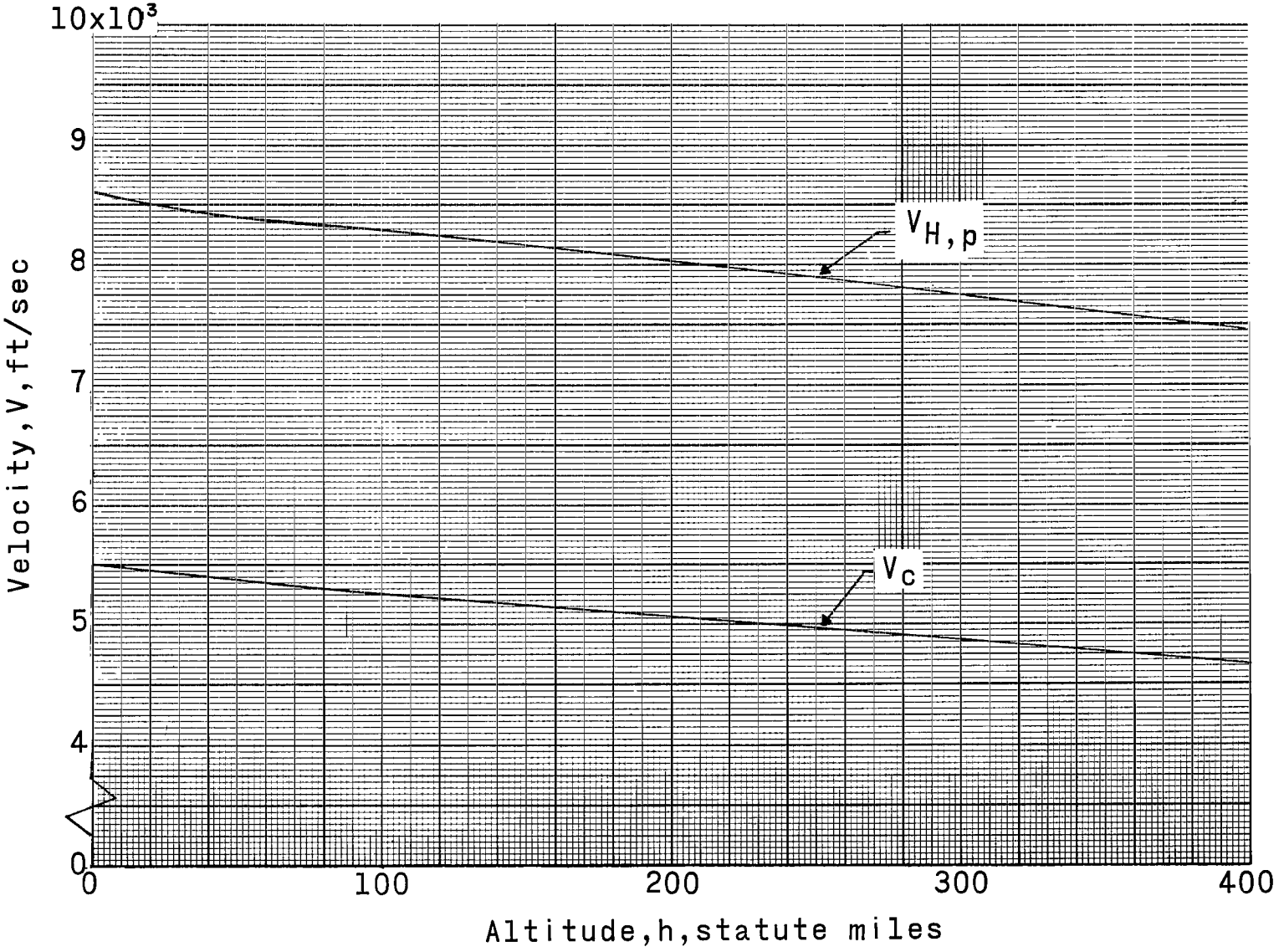

Figure 4.- Pericynthion velocity for 60-hour hyperbolic lunar trajectory and circular velocity as a function of altitude.

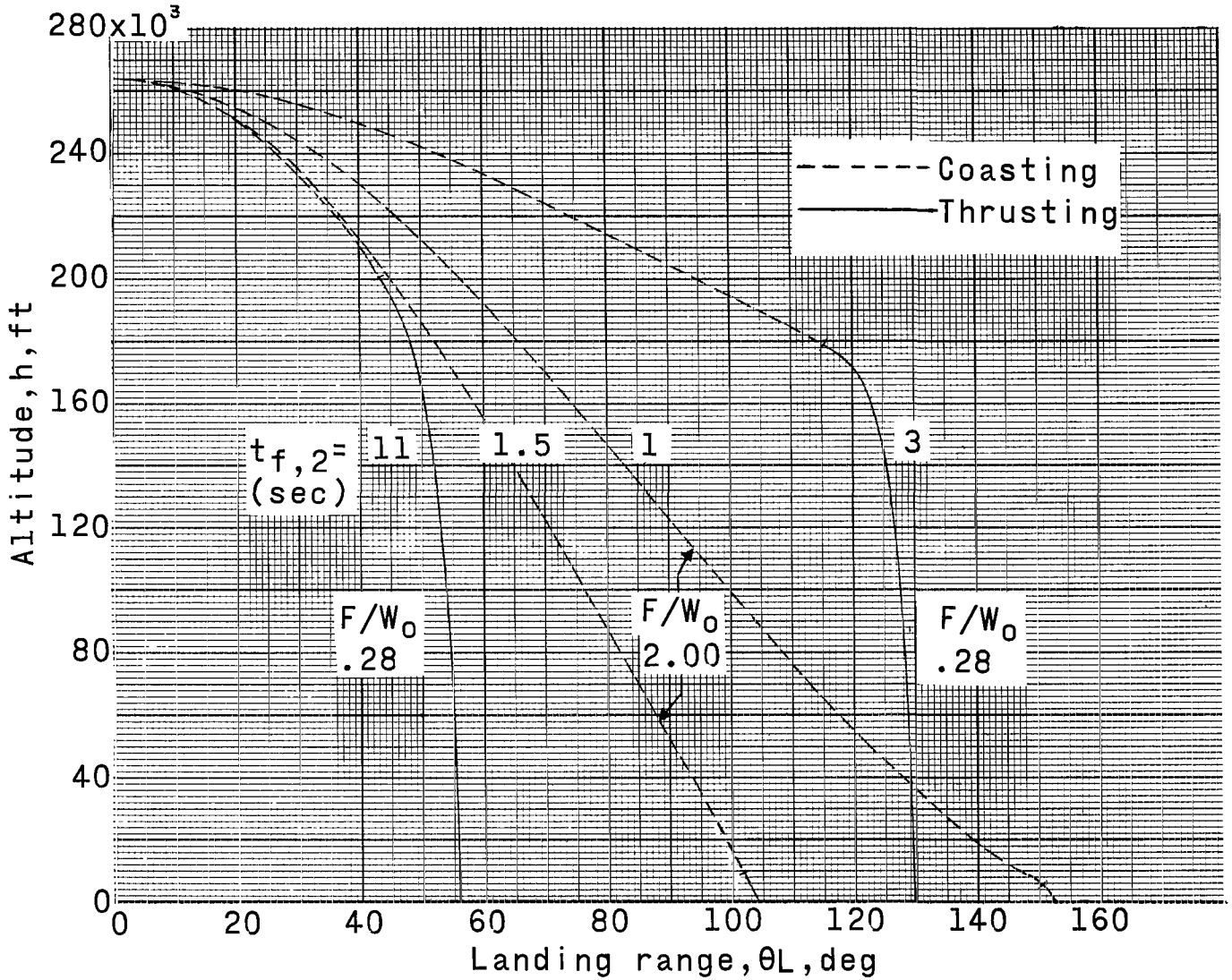

(a) 50-mile-altitude parking orbit.

Figure 5.- Variation of altitude with landing range for various initial thrust-weight ratios and deorbiting thrusting periods.

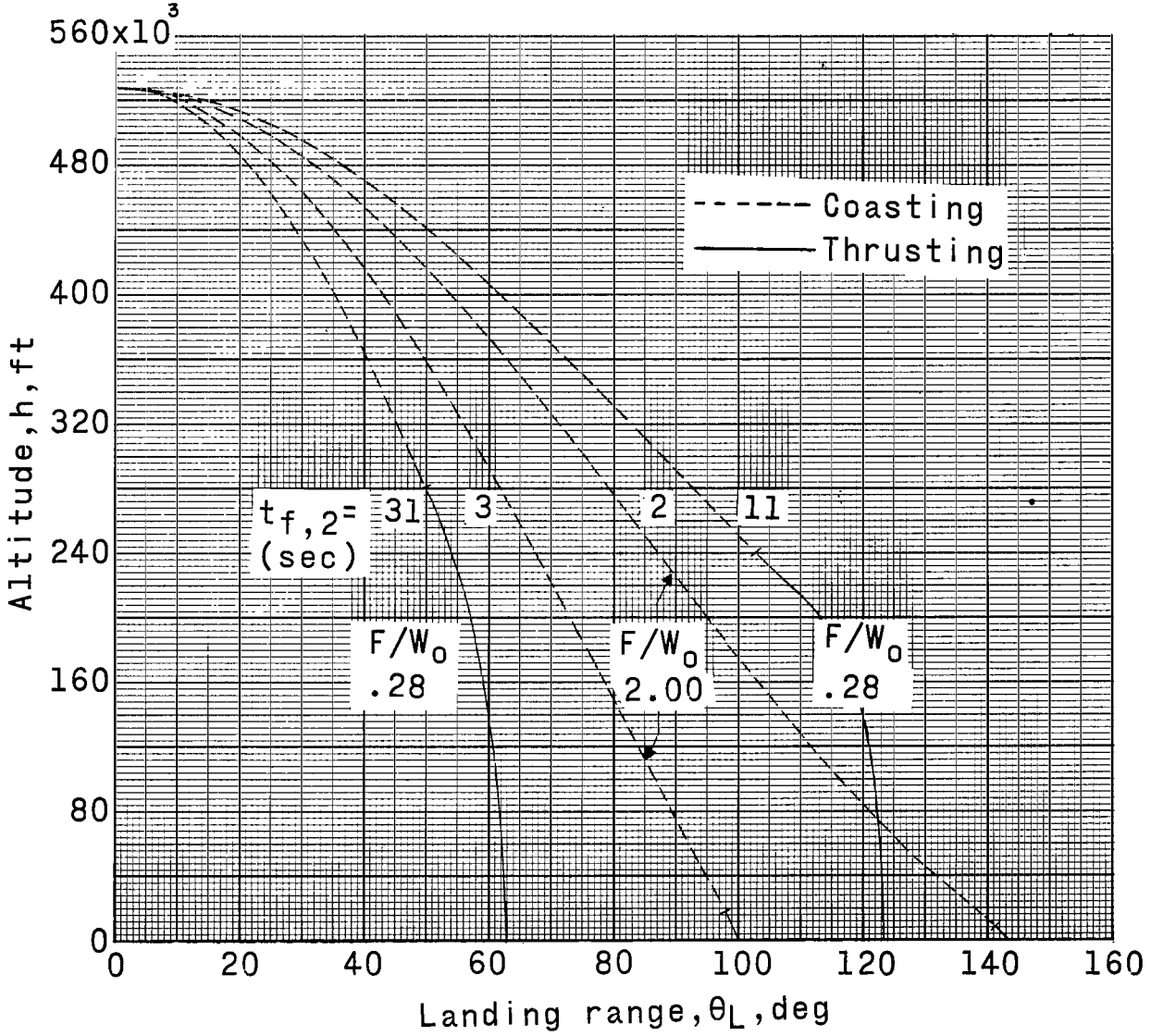

(b) 100-mile-altitude parking orbit.

Figure 5.- Concluded.

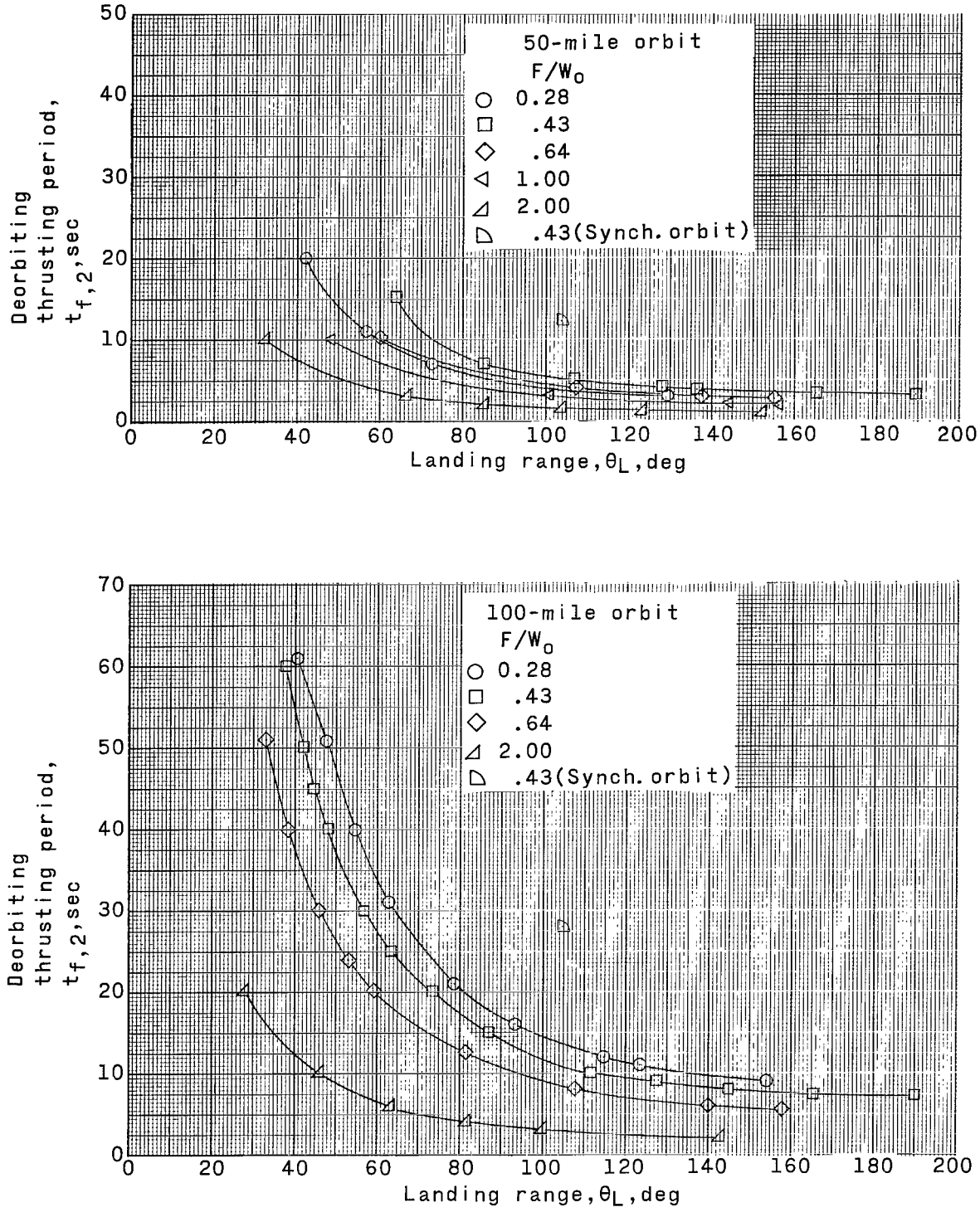

Figure 6.- Effect of deorbiting thrusting period on angular range for various initial thrust-weight ratios.

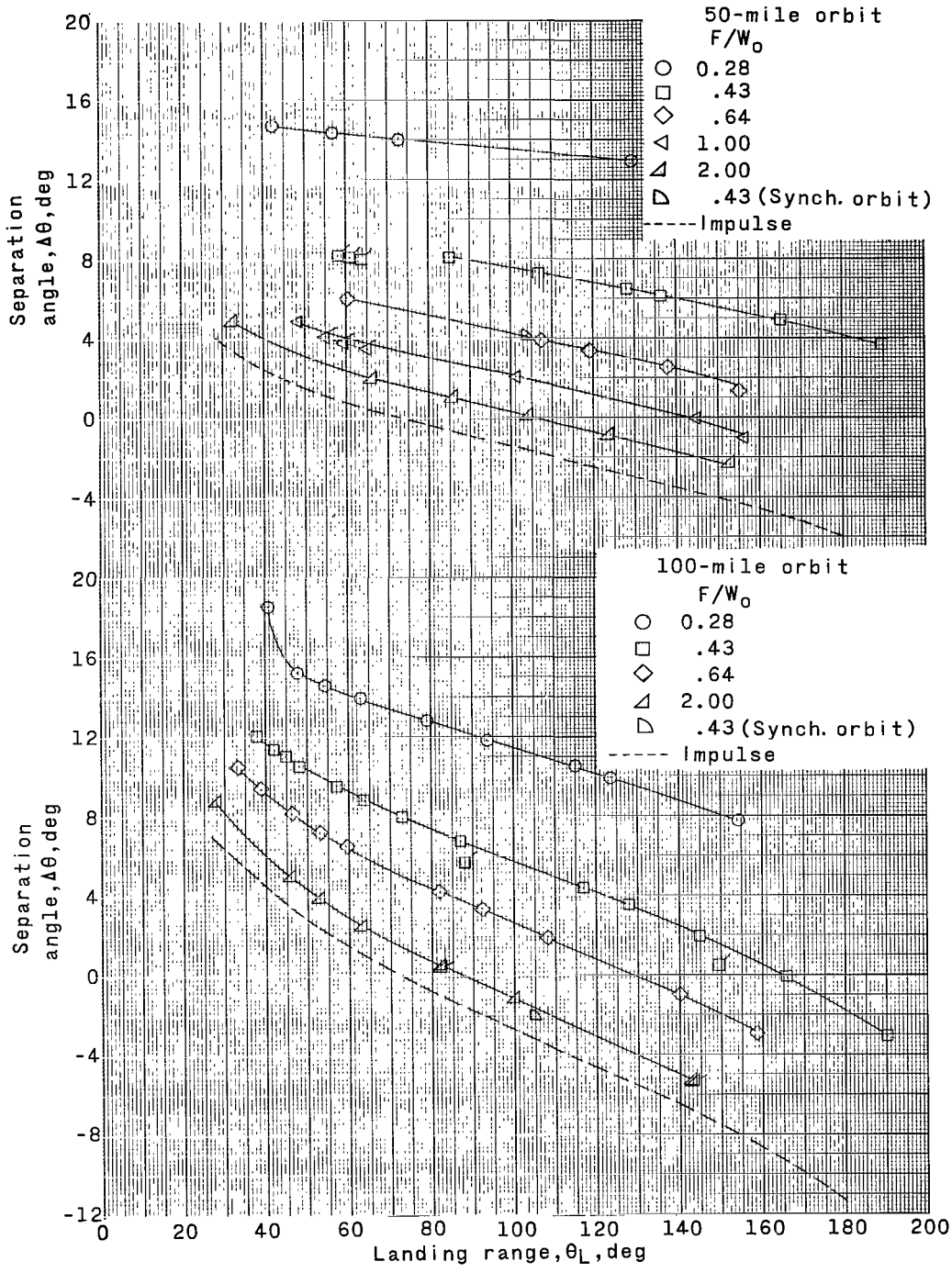

Figure 7.- Separation angle between lunar excursion module and orbiter at module touchdown for several initial thrust-weight ratios. Ticked symbols indicate a specific impulse of 310 seconds.

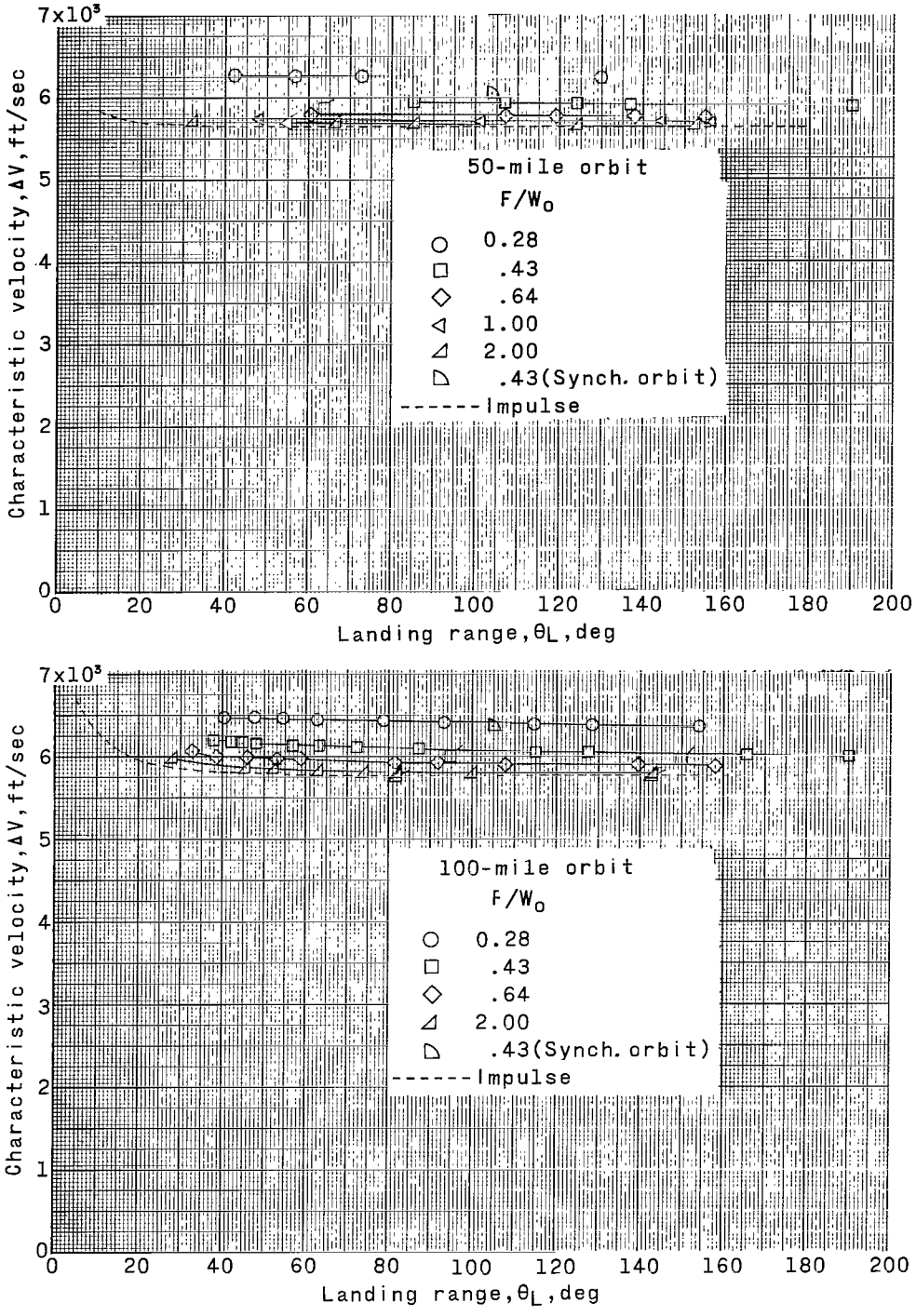

Figure 8.- Characteristic velocity as a function of initial thrust-weight ratio for 50- and 100-mile-altitude parking orbits. Ticked symbols indicate a specific impulse of 310 seconds.

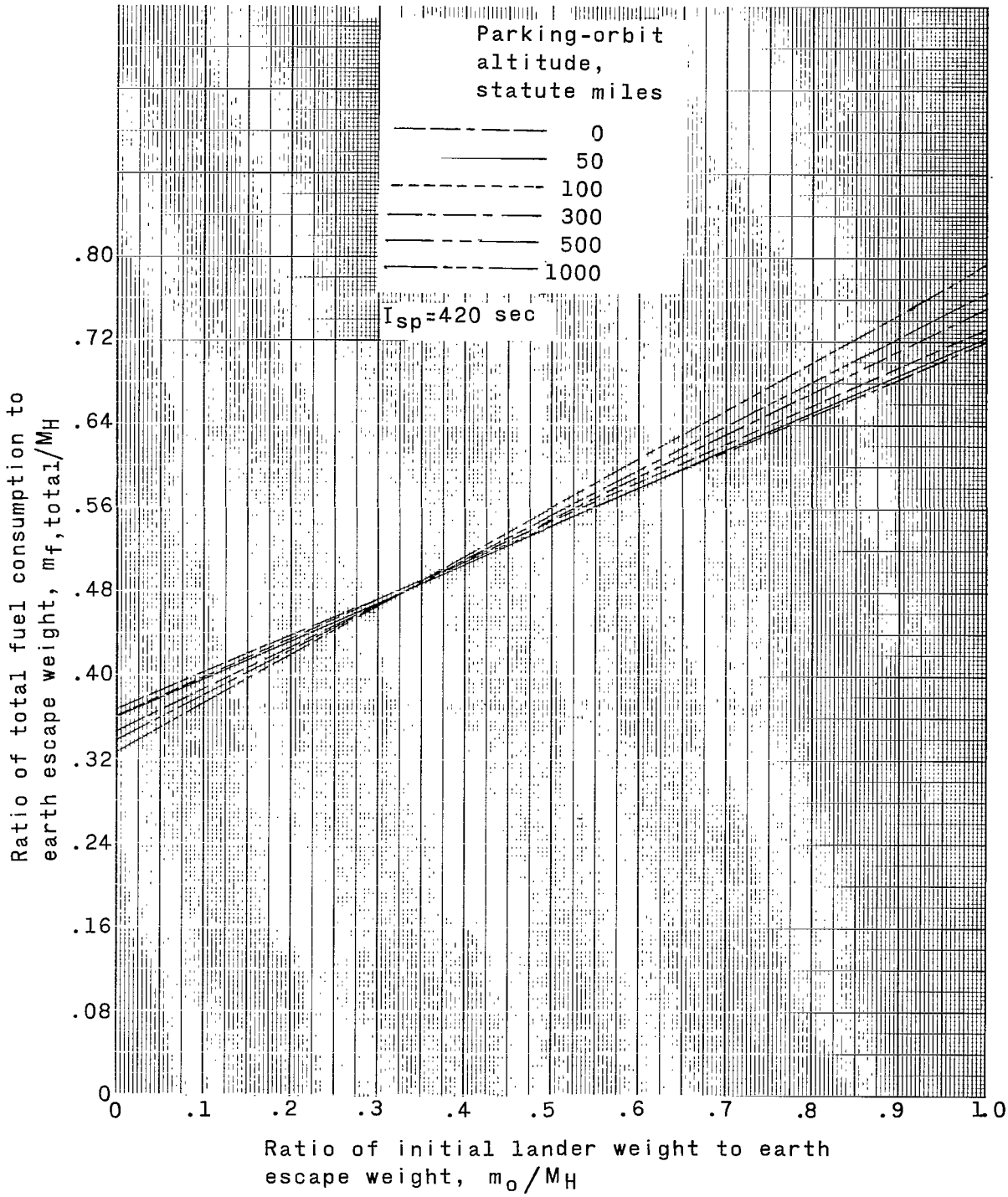

Figure 9.- Impulsive fuel consumption as a function of lunar-excursion-module weight and various parking-orbit altitudes. Calculations were made by use of a Hohmann transfer.

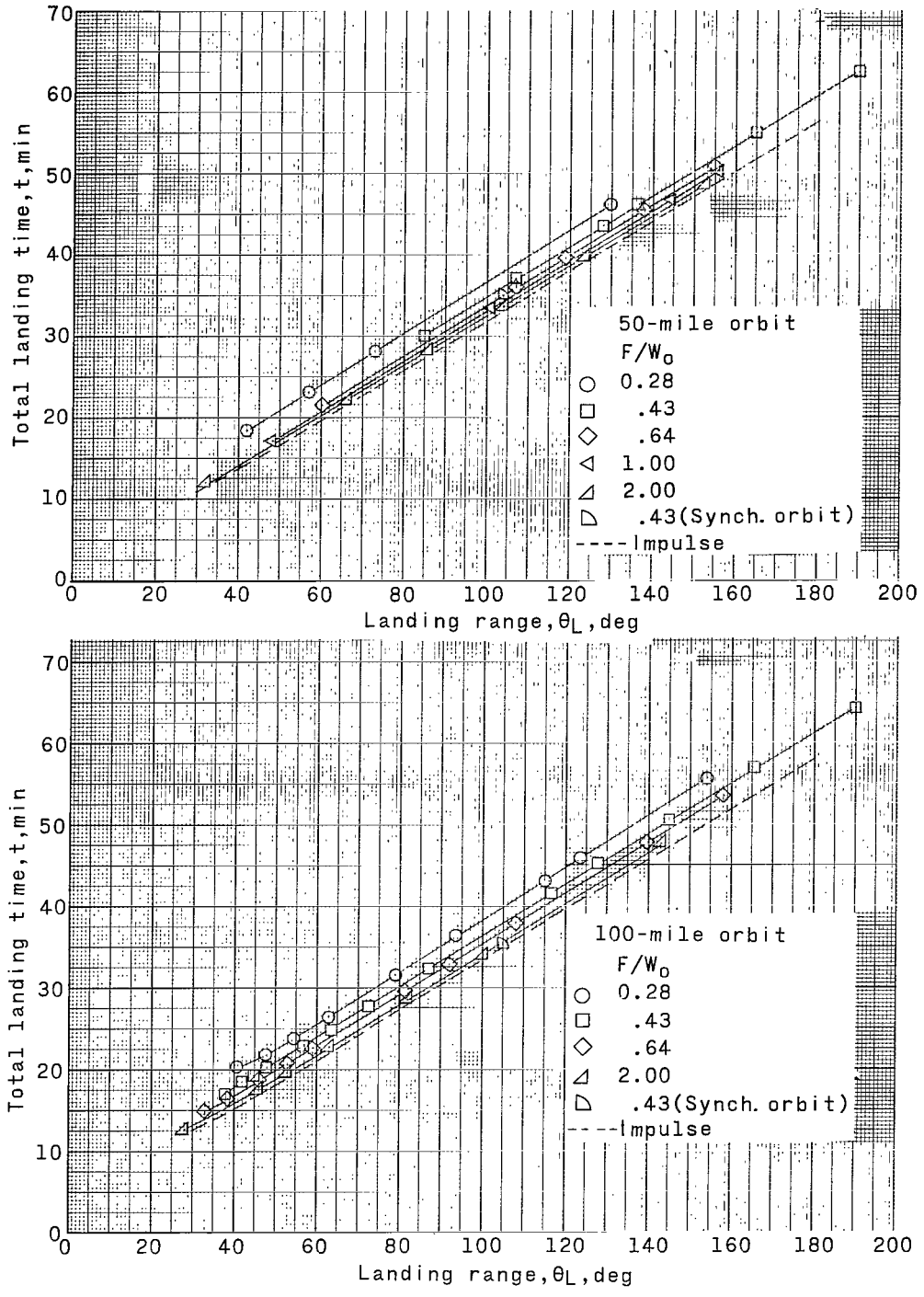

Figure 10.- Variation of total landing time with angular travel over lunar surface for various initial thrust-weight ratios.

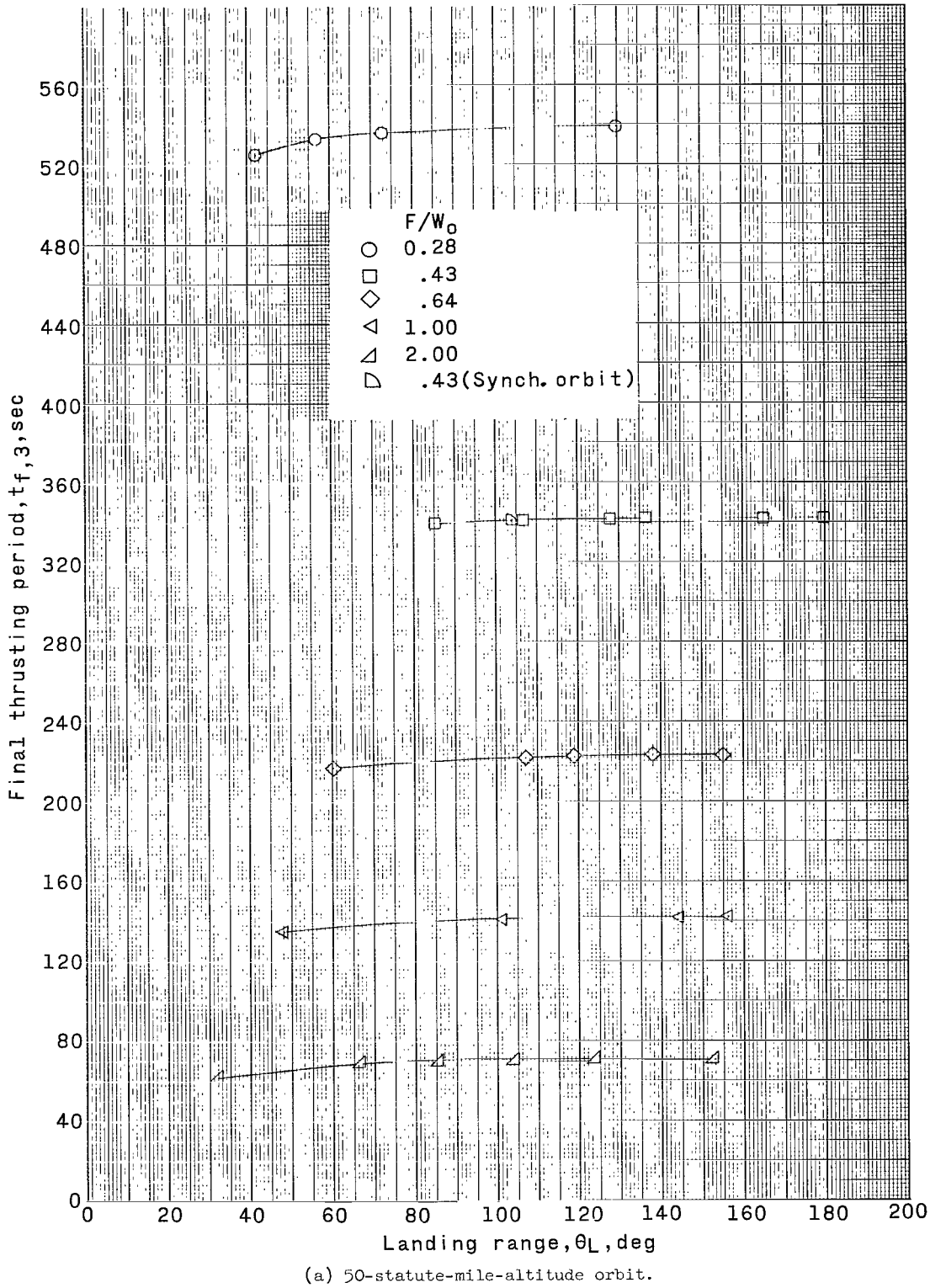

(a) 50-statute-mile-altitude orbit.

Figure 11.- Final thrusting period as a function of angular travel over the lunar surface for values of initial thrust-weight ratio.

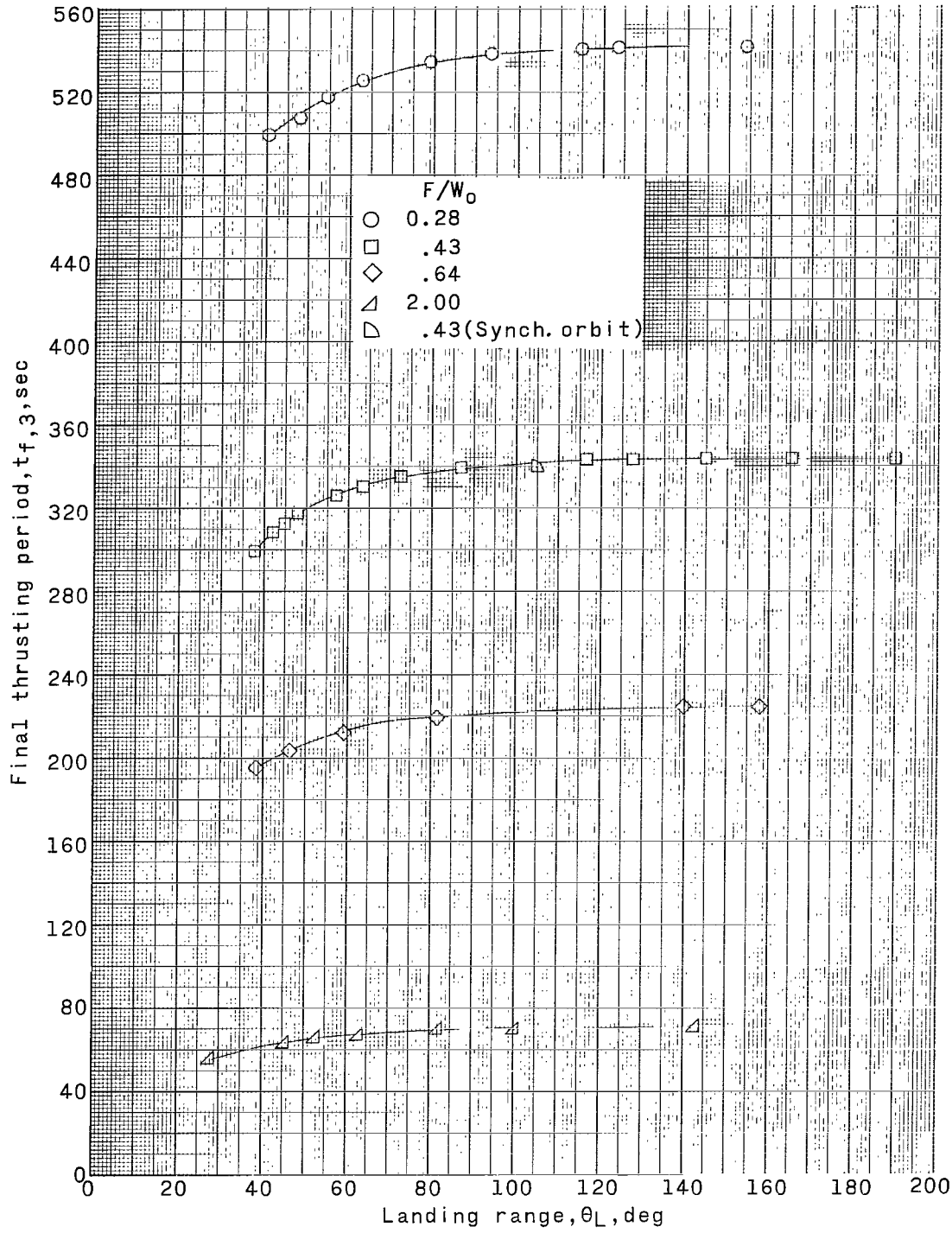

(b) 100-statute-mile-altitude orbit.

Figure 11.- Concluded.

NASA-Langley, 1963 L-3403